Carbon nanotube grafted carbon fibres: a study of wetting and fibre fragmentation

Hui Qian[1,2], Alexander Bismarck[2], Emile S. Greenhalgh[3], Milo S.P. Shaffer[1,*]

[1] Department of Chemistry, Imperial College London, London SW7 2AZ, UK
[2] Polymer and Composite Engineering (PaCE) Group, Department of Chemical Engineering, Imperial College London, London SW7 2AZ, UK
[3] The Composites Centre, Imperial College London, London SW7 2AZ, UK

Abstract

Carbon nanotubes (CNTs) were grafted on IM7 carbon fibres using the chemical vapour deposition method. The overall grafting process resulted in a threefold increase of the BET surface area compared to the original primary carbon fibres (0.57 m^2/g). At the same time, there was a degradation of fibre tensile strength by around 15% (depending on gauge length), due to the dissolution of iron catalyst into the carbon; the modulus was not significantly affected. The wetting behaviour between fibres and poly(methyl methacrylate) (PMMA) was directly quantified using contact angle measurements for drop-on-fibre systems and indicated good wettability. Single fibre fragmentation tests were conducted on hierarchical fibre/PMMA model composites, demonstrating a significant (26%) improvement of the apparent interfacial shear strength (IFSS) over the baseline composites. The result is associated with improved stress transfer between the carbon fibres and surrounding matrix, through the grafted CNT layer. The improved IFSS was found to correlate directly with a reduced contact angle between fibre and matrix.

Keywords: A. Carbon fibre; A. Hybrid; A. Nano-structures; B. Interface/interphase.

[*] Corresponding author. Tel.: +44 (0)20 7594 5825; Fax.: +44 (0)20 7594 5801; E-mail address: m.shaffer@imperial.ac.uk (M. S. P. Shaffer).

1. Introduction

Since the 1960s, fibre-reinforced polymer composites have made a huge impact, particularly in the aerospace and oil/gas industries [1]. Compared to their excellent in-plane properties, the relatively weak compression and interlaminar properties remain major issues [2]. Meanwhile, there is a growing body of evidence that carbon nanotubes (CNTs) are ideal candidates for reinforcement in composite materials due to their nanoscale structure, outstanding mechanical, thermal and electrical properties [3-5]. Therefore, consideration has been given to introducing CNTs into conventional fibre reinforced composites, forming a hierarchical structure, where nanoscale reinforcement is made to work alongside a more traditional microscale architecture.

One promising opportunity is to incorporate CNTs into the matrices of conventional fibre reinforced composites [6-10], in order to address the critical matrix-dominated failure mechanisms, such as those mentioned above. However, earlier studies [6, 8] showed that attempts to infiltrate CNT-based resins, for example by vacuum assisted resin transfer moulding, are severely limited by viscosity and self-filtration issues that related to the presence of the CNTs. In addition, the flow of the resin during impregnation tends to align the CNTs parallel to the primary fibres, the least desirable orientation for enhancing the matrix-dominated composites performance. On the other hand, interest is rapidly growing in hierarchical CNT-grafted fibre/polymer composites. By grafting CNTs onto fibre surfaces, there is a potential to provide a high loading of radially-aligned CNTs that is expected to be optimal for transverse reinforcement. This grafting method also alleviates the problem of agglomeration commonly observed when CNTs are freely dispersed in the resin. In addition, the presence of the CNTs on the fibre surface can improve the interfacial properties between fibres and matrix, and potentially enhance associated properties, such as delamination resistance, transverse

tension and longitudinal compression strengths. Such reinforcement, radial to the fibres and extending into the surrounding matrix, is likely to stiffen the matrix and provide increased lateral support of the load-bearing fibres. In principle, an inhibition of fibre microbuckling would translate into considerable enhancements in longitudinal compression performance, recognised as a significant hurdle in primary structural applications [11]. Finally, the CNTs may introduce additional damage processes which would enhance the local toughness of the matrix during fracture.

A number of studies have reported the fabrication of CNT-grafted fibres using both direct growth of CNTs onto fibres [12-19] and chemical reactions between modified fibres and CNTs [20]. Among those methods, chemical vapour deposition (CVD) appears to be an efficient way to produce CNT-grafting, with controllable size [16, 21] and orientation [14]. Some positive results [15, 18, 19] have been reported on the improvement of critical mechanical properties of hierarchical composites with CNT-grafted fibres, including increased interlaminar shear strength [18], delamination resistance [15, 19], and hardness [15]. Improvement in interfacial properties have also been reported using this type of hierarchical structure [12, 17, 22, 23].

It is well known that the performance of fibre reinforced polymer composites is strongly dependent on the interfacial properties, specially the adhesion between fibres and matrix, which relates both to the wettability of fibres by the polymer and the interfacial shear strength (IFSS). In the present study, the influence of the CNT-grafting on the wetting behaviour between carbon fibres and a polymer matrix was explored using direct contact angle measurements. The wetting issue, together with the change of surface area, was related to the interfacial performance of model composites, which was studied using single fibre fragmentation tests. In addition, the tensile properties of the carbon fibres after different modifications were compared with the literature values.

2. Experimental

2.1. Materials

Commercially-available, unsized, polyacrylonitrile (PAN)-based IM7 carbon fibres (Hexcel Composites) were used for this study. Earlier work of CNT growth on C320.00A (C320) carbon fibres (Sigri, SGL-Carbon AG) [17] showed that the pre-treatment of fibres, which involved a 5h acid oxidation, is crucial for obtaining uniform deposition of catalyst. Therefore, the carbon fibres were oxidised using a wet chemical method [24], involving an acid oxidation (65% HNO_3, Aldrich), followed by a base wash (NaOH, Aldrich), for 24 h. However, in order to study the effects of fibre pre-treatment on the CNT grafting, shorter oxidation time, i.e. 30 min, was used for IM7 carbon fibres. PMMA (PLEXIGLAS® zk6BR, Evonik Röhm GmbH) was selected as the matrix for single fibre fragmentation tests, which requires a relatively high strain at break. Wetting experiments were performed using the same matrix, in order to explore the relationship between IFSS and contact angle. All chemicals were used as-received.

2.2. Grafting CNTs onto carbon fibres

An incipient wetness technique was employed to load iron catalyst on the fibre surfaces prior to the CVD synthesis of CNTs [17, 25]. The iron catalyst was introduced onto oxidised carbon fibres by immersing the fibres into a 100 mM ethanol solution of $Fe(NO_3)_3 \cdot 9H_2O$ (A.C.S reagent, Aldrich) and rinsing with distilled water. The growth of CNTs was performed in a tubular quartz furnace (~ 50 mm in diameter) by using acetylene (C_2H_2) as the hydrocarbon source in the CVD reaction. A 10% H_2/Ar mixture was used as the carrier gas. The reactions were performed at 750 °C for 1 h, using a 1:300 flow ratio of C_2H_2 to carrier gas.

The modified carbon fibres were characterised using a field emission gun scanning electron microscope (Gemini LEO 1525 FEG-SEM, Carl Zeiss NTS GmbH).

2.3. BET surface area measurements

The specific BET surface area of carbon fibres was measured by nitrogen adsorption (oxygen-free N_2, BOC, UK), according to ISO 9277, using a Micromeritics TriStar 3000 analyser.

2.4. Single fibre tensile tests

Single fibre tensile tests were carried out at ambient temperature at a crosshead speed of 15 μm/s, according to the standard BS ISO 11566:1996 using a TST 350 tensile testing rig (Linkam Scientific Instrument Ltd.) equipped with a 20 N load cell. A single fibre was glued at either end onto a small piece of cardboard for better handling. The gauge lengths were 15, 25 and 35 mm. A minimum of twenty measurements were conducted for each fibre specimen at each gauge length. The system compliance, C , was estimated to be 0.4 mm/N under the relevant experimental conditions. The apparent elastic modulus was therefore corrected using the following equation (BS ISO 11566:1996 Method B):

$$E = E^* \Big/ \left(1 - C\,\frac{E^* A}{L}\right) \tag{1}$$

where C is the system compliance, E^* is the apparent modulus, derived from the gradient of the stress-strain curve, A is the cross-sectional area of the fibre, and L is the gauge length.

2.5. Contact angle measurements

The wettability of carbon fibres by PMMA was quantified directly in a drop-on-fibre system using the generalized drop length-height method [26, 27]. Single fibres were glued to a metal washer using an epoxy adhesive (Adhesive weld, J-B Weld, Slough) and dipped into PMMA powder. The specimen was then transferred into a hot stage (THM600, Linkam Scientific Instrument Ltd.) and heated to 270ºC, at which

temperature PMMA possessed liquid-like behaviour. Stable polymer droplets were formed on the fibres after 45 mins and images were captured using an Olympus DP70 camera system under an Olympus BH-2 optical microscope. The droplet profiles were extracted and contact angles were determined (specific methodology available elsewhere [26]) from at least 50 droplets, on at least three fibres, for each type of carbon fibre, in order to obtain statistically significant averages.

2.6. Single fibre fragmentation tests

Single fibres were glued at either end to glass slides by using double sided tape with a defined thickness of approximately 100 μm. By doing this, the fibres were kept away from surfaces of glass slides and positioned in the centre of the polymer specimens. A 10 wt.% solution of PMMA in 1,4-dioxane (Sigma-Aldrich) was prepared and cast onto the glass slides, covering the fibres completely. The films were first dried for 48 h in a fume hood and for a further 24h in a vacuum oven to remove any trace of solvent. Dogbone shaped specimens were then cut using the Zwick D-7900 cutting device (Zwick Roell Group) and tested on the TST 350 tensile stress testing system (Linkam Scientific Instrument Ltd.). The dimensions of the specimens tested were approximately 0.2 mm thick, 4 mm wide (at gauge region) and 30 mm long. During the tests, the specimens were strained up to 25% to ensure crack saturation, at a crosshead speed of 15 μm/s, and the entire single fibre fragmentation process was monitored via polarized light microscope (Wild Heerbrugg). At least six specimens were tested for each case. The fibre fragment lengths were measured using an Olympus BX51M reflected light optical microscope with an Olympus DP70 camera system, which was calibrated using a glass scale (10mm Stage Micrometer Scale, 0.1mm divisions, Graticules Ltd.). The apparent interfacial shear strength, τ_{IFSS} , can be estimated from the Kelly-Tyson model [28]:

$$\tau_{IFSS} = \frac{\sigma_f d_f}{2 l_c} \quad (2)$$

$$l_c = \frac{4}{3} l \quad (3)$$

where d_f is the fibre diameter, σ_f is the fibre strength at the critical fragment length, l_c, which can be obtained from the mean fibre fragment length, l, at crack saturation [29].

2.7. Fractographic analysis

The carbon fibre/PMMA composite specimens, which had been measured using the single fibre fragmentation tests, were broken in flexure, perpendicular to the fibre direction, to expose translaminar fractures. For further fractographic analysis of carbon fibre/epoxy composites, fibres were laid flat into a small mould; epoxy resin (HexPly 8552, Hexcel Composites) was introduced and cured. The specimens were then fractured in flexure, transverse to the fibres, to generate intralaminar fracture surfaces, parallel to the fibre orientation. All the specimens were gold-coated for 2 minutes by sputter coating (K-550X, Emitech Ltd.) before SEM analysis.

3. Results and discussion

3.1. CNT grafting on fibres

After performing the incipient wetness technique, it was apparent that iron particles, with diameters in a range of 20 to 45 nm (mean value around 30 nm), were uniformly deposited onto the fibre surfaces (Fig. 1b), with a surface density of around 10^{14} m^{-2}. These iron catalyst particles resulted in a homogeneous growth of randomly-oriented, curly multi-walled CNTs that appear typical of CVD growth. Traditional Raman or X-ray analysis of the CNT crystallinity is not straightforward against the background of the underlying carbon fibre, but these CNTs can be expected to be tubular and moderately defective, giving rise to the observed curvature. The diameters were

between 20 and 50 nm (mean value around 30 nm), and lengths were a few micrometres (Fig. 1e-f). As expected, the catalyst particles were a similar diameter to the CNTs grown from them [30]. The initial oxidation of the carbon fibres before catalyst deposition is crucial; the oxygen-containing groups present after acid treatment encourage the wetting of fibres by the aqueous salt solutions and help to stabilise small iron particles on the surface during the initial catalyst deposition [17].

3.2. BET surface area measurements

A slight increase in the BET surface area was observed for the oxidised IM7 carbon fibres, from 0.57 to 0.71 m^2/g, as expected due to etching of the surface [31]. However, the BET surface area increased further to 1.71 m^2/g after CNT grafting; based on an average outer diameter of 30 nm, this surface area increase implies a CNT grafting density around 0.015 g/m^2. Similar increases in surface area were observed for CNT-grafted C320 carbon fibres, but the relative magnitude of the effect was bigger (from 0.24 to 1.60 m^2/g, indicating a grafting density around 0.07 g/m^2). Variations in the oxidation time and the underlying carbon microstructure, gave rise to a higher grafting density in that case; note also that the initial diameter of the C320 carbon fibres was larger and hence the absolute surface area was smaller.

3.3. Single fibre tensile tests

Typically, extensive oxidation of carbon fibres is known to cause significant reductions in tensile strength[24, 32]; however, in certain circumstances, increases have been reported, presumably associated with the removal of surface defects. In the present case, a slight increase (around 7%) of the fibre strength was detected after the oxidation step (Fig. 2), indicating the intrinsic fibre strength may be maintained at short oxidation times, for example, no more than 30 minutes under the current conditions. After the CNT growth, the fibre strength dropped by around 15-17%, depending on gauge length

(see Table 1). This degradation was mainly attributed to the dissolution of iron catalyst into the carbon fibres at the reaction temperature, which was above the iron-carbon eutectic temperature of 723°C [33]. The strength loss reported in earlier work [17] was around 55% for C320 carbon fibres. The greater degradation in the previous case correlates with the higher CNT grafting density, although variations in the graphite microstructure and intrinsic properties of the pristine fibres may also play a role.

It is widely accepted that the tensile strength of carbon fibres has a length dependence due to the defect-induced nature of fibre failure [34]. As clearly shown in Fig. 2a, the average strengths of all the carbon fibres decreased with increasing gauge length. In order to account for the length dependence, a Weibull distribution [35] was fitted to the experimental data; the similarity of the gradients indicates that the surface damage was relatively uniform along the fibres. On the other hand, the tensile modulus of the fibres was almost unaffected (Fig. 2b), suggesting the fibre core remained undamaged during the modifications.

3.4. Contact angle measurements

Typical micrographs of PMMA droplets formed on different carbon fibres are shown in Fig. 3, all showing barrel-type droplets, which is the preferred configuration when the contact angle is relatively small (usually clam-type droplet is characteristic of poor wetting with contact angles larger than 60°) [36, 37]. It is generally accepted that axially symmetric, barrel-type polymer droplets can be formed on fibres that possess good wettability by the polymer, due to the geometrical constraints of a Laplace ellipsoid on a cylindrical fibre [38, 39]. By oxidising the surfaces of carbon fibres, the contact angle decreased slightly from 27.4 $\pm$ 0.8° to 25.7 $\pm$ 0.8°, which could be attributed to the additional surface oxides after the acid treatment. The contact angle dropped to 21.6 $\pm$ 0.7° after growing the CNTs, indicating a good wettability by PMMA. The result is

perhaps surprising from a chemical perspective but can be explained by considering roughness. As mentioned above, the grafting process gave rise to a significant increase in surface area, i.e., roughness of the pristine carbon fibres. Surface roughness plays an important role in the wettability of a surface and the impact of roughness on the contact angle can be described by the Wenzel equation [40]:

$$\cos(\theta_r) = r\cos(\theta_s) \quad (4)$$

where r is the roughness factor, defined as the ratio between the actual surface area of a rough surface to the projected one; θ_s and θ_r are the apparent contact angles on the smooth and rough surfaces, respectively. Wenzel's relation shows that the roughening effect ($r > 1$) enhances either the wetting or the non-wetting properties of the solid–liquid system, depending on whether θ_s is smaller or greater than 90° [41, 42]. As the carbon fibres were wettable by the polymer melt, a decrease in contact angle is expected in this case. The roughness factor of the CNT-grafted fibres, estimated based on the measured BET surface areas is around 4. Theoretically, this large increase in roughness could lead to a more significant decrease of the apparent contact angle than observed; however, the CNTs are more hydrophobic than the oxidised carbon fibre surface (even after the growth process) [17], resulting in a more modest improvement in wetting.

3.5. Single fibre fragmentation tests

The interfacial properties of fibre/PMMA model composites were investigated further, using single fibre fragmentation tests (Fig. 4). The morphology associated with the fibre breaks can offer valuable clues regarding the interface strength [43]. The composite specimens with as-received carbon fibres exhibited apparent debonding at the interface and no damage in the matrix around the fibre breaks (Fig. 4a), implying a relatively weak interface. Significant interface debonding was also observed for the composites containing oxidised carbon fibres (Fig. 4b). By grafting fibre surfaces with CNTs, the

failure of the composite specimen indicated a moderately strong interface bond, with a mixture of break widening and apparent local deformation of the matrix (Fig. 4c).

The histogram of fragment lengths (Fig. 5a) showed that the composite specimens with CNT-grafted fibres displayed shorter fragment lengths than those with bare carbon fibres, resulting in a shift to lower fragment length in the cumulative distributions (Fig. 5b). The change of the curve shape in the cumulative distributions can be attributed to differences in fibre strength variability [43]. With constant fibre strength, shorter fragment length normally indicates better fibre/matrix adhesion. However, the CNT grafting process resulted in a change of the fibre strength, as demonstrated in the single fibre tensile tests. Therefore, a quantitative study of the interfacial shear strength was carried out using the Kelly-Tyson model [28] and the Weibull fitting to predict the fibre tensile strength at the critical length (Table 1). The oxidation of carbon fibres gave rise to a slight increase of the IFSS (about 5%), which can be expected given the slight changes of surface area and contact angle. By grafting the carbon fibres with CNTs, the IFSS increased by around 26%, which can be attributed to the increased surface area, good wettability and mechanical interlocking of CNTs. The increased IFSS correlated well with the reduced direct wetting contact angles (Fig. 6). Presumably, with variations of the grafting parameters, such as catalyst deposition and growth time, higher loadings of CNTs could be obtained on carbon fibres, which should lead to further improvements in the interfacial properties.

3.6. Fractographic analysis

The revealed cross-sections of the fragmentation specimens were characterised using SEM and the typical fracture surfaces are shown in Fig. 7. It is clear that the fracture planes initiated at the interface between fibre and matrix, regardless of the CNT-grafting. This observation suggests that the fracture mode of IM7 carbon fibre/PMMA

composites is unaffected by the CNT grafting. In contrast, a cohesive fracture mechanism was observed in an earlier fractographic study of CNT-grafted C320 carbon fibre/epoxy composites [17]; the failure plane was within the fibres rather than at the interface, and the outer layers of the fibres were peeled off during the fracture process, due to the fibre strength degradation. As a comparison, model composites with IM7 carbon fibres in epoxy (HexPly® 8552, Hexcel Composites) were fabricated to study the transverse (intralaminar) fracture surfaces (Supplementary material, Fig. S1). Similar fracture morphology to the PMMA composites was observed, exhibiting relatively smooth fibre surfaces and fracture planes between fibres and matrix. The diameter of the carbon fibres was unchanged after the fracture, demonstrating that no cohesive fracture had occurred in this case. The different fracture behaviour between the two types of carbon fibres could be related to variations in intrinsic microstructure, CNT grafting density, or surface damage during the grafting reaction. It's worth noting that the tensile strength of the C320 carbon fibres (~ 1590 MPa) was much lower than that of IM7 (~ 4670 MPa) after CNT grafting.

4. Conclusions

CNT-grafted IM7 carbon fibres were fabricated using the CVD method. The grafting process resulted in an apparent increase of the BET surface area and a moderate decrease of the fibre tensile strength. The degradation can be attributed to the dissolution of iron particles into the carbon fibre surface during the high temperature growth reaction, but was less significant than in previous studies. The results suggest that, by optimising the fibre pre-oxidation and CNT grafting density, an improved IFSS might be obtained with minimal degradation of the primary tensile fibre properties. Contact angles between carbon fibres and PMMA were directly quantified using a drop-on-fibre method and demonstrate that the CNT grafting possesses good wettability by

the polymer. The IFSS increased significantly after CNT grafting, by around 26%, in a manner that was found to correlate with the contact angle measurements. The IFSS values obtained in the current study were derived from fragmentation tests, rather than single fibre pull-out or push-out tests, and appear to be less susceptible to loading artefacts. These single fibre level results are encouraging, and support further development of the approach to a larger scale. Given that high performance IM7 carbon fibres are widely used in aerospace and F1 applications, for example in A350 and JSF, the findings of this paper suggest that existing (aerospace qualified) composite systems could be enhanced using CNT grafting technology. In principle, the methodology should yield CNT-grafted fibres suitable for improving critical engineering properties of conventional composites, such as interlaminar toughness and compression strength. In addition, the reported high thermal and electrical conductivity of CNTs could confer the composite materials with secondary characteristics that will make them attractive for application to a wide range of structures and platforms.

Acknowledgements

The authors would like to thank DSTL and QinetiQ for the financial support of this work and Hexcel for supplying the IM7 carbon fibres and epoxy resin.

Reference

[1] Bunsell AR, Renard J. Introduction. Fundamentals of fibre reinforced composite materials: Taylor & Francis 2005:1-17.

[2] Tong L, Mouritz AP, Bannister M. Introduction. 3D Fibre Reinforced Polymer Composites: Elsevier Science, Oxford 2002:1-12.

[3] Shaffer M, Sandler J. Carbon Nanotube/Nanofibre Polymer Composites. In: Advani SG, ed. Processing and Properties of Nanocomposites: New Jersey, NJ [etc.] : World Scientific 2007:1-59.

[4] Coleman JN, Khan U, Blau WJ, Gun'ko YK. Small but strong: A review of the mechanical properties of carbon nanotube-polymer composites. Carbon. 2006;44:1624-52.

[5] Harris P. Carbon nanotube composites. International Materials Reviews. 2004;49(1):31-43.

[6] Fan ZH, Hsiao KT, Advani SG. Experimental investigation of dispersion during flow of multi-walled carbon nanotube/polymer suspension in fibrous porous media. Carbon. 2004;42:871-6.

[7] Gojny FH, Wichmann MHG, Fiedler B, Bauhofer W, Schulte K. Influence of nano-modification on the mechanical and electrical properties of conventional fibre-reinforced composites. Compos Part A: Appl Sci Manuf. 2005;36(11):1525-35.

[8] Sadeghian R, Gangireddy S, Minaie B, Hsiao KT. Manufacturing carbon nanofibers toughened polyester/glass fiber composites using vacuum assisted resin transfer molding for enhancing the mode-I delamination resistance. Compos Part A: Appl Sci Manuf. 2006;37(10):1787-95.

[9] Qiu JJ, Zhang C, Wang B, Liang R. Carbon nanotube integrated multifunctional multiscale composites. Nanotechnology. 2007;18(27):275708.1-11.

[10] Fan ZH, Santare MH, Advani SG. Interlaminar shear strength of glass fiber reinforced epoxy composites enhanced with multi-walled carbon nanotubes. Compos Part A: Appl Sci Manuf. 2008;39(3):540-54.

[11] Pinho ST, Robinson P, Iannucci L. Fracture toughness of the tensile and compressive fibre failure modes in laminated composites. Compos Sci Technol. 2006;66(13):2069-79.

[12] Thostenson ET, Li WZ, Wang DZ, Ren ZF, Chou TW. Carbon nanotubes/carbon fiber hybrid multiscale composites. J Appl Phys. 2002;91:6034-7.

[13] Zhu S, Su CH, Lehoczky SL, Muntele I, Ila D. Carbon nanotube growth on carbon fibers. Diamond Relat Mater. 2003;12:1825-8.

[14] Boskovic BO, Golovko VB, Cantoro M, Kleinsorge B, Chuang ATH, Ducati C, et al. Low temperature synthesis of carbon nanofibres on carbon fibre matrices. Carbon. 2005;43:2643-8.

[15] Veedu VP, Cao AY, Li XS, Ma KG, Soldano C, Kar S, et al. Multifunctional composites using reinforced laminae with carbon-nanotube forests. Nat Mater. 2006;5(6):457-62.

[16] Zhao JO, Liu L, Guo QG, Shi JL, Zhai GT, Song JR, et al. Growth of carbon nanotubes on the surface of carbon fibers. Carbon. 2008 Feb;46(2):380-3.

[17] Qian H, Bismarck A, Greenhalgh ES, Kalinka G, Shaffer MSP. Hierarchical composites reinforced with carbon nanotube grafted fibers: The potential assessed at the single fiber level. Chem Mater. 2008 Mar;20(5):1862-9.

[18] Garcia EJ, Wardle BL, Hart AJ, Yamamoto N. Fabrication and multifunctional properties of a hybrid laminate with aligned carbon nanotubes grown In Situ. Compos Sci Technol. 2008 Jul;68(9):2034-41.

[19] Kepple KL, Sanborn GP, Lacasse PA, Gruenberg KM, Ready WJ. Improved fracture toughness of carbon fiber composite functionalized with multi walled carbon nanotubes. Carbon. 2008;46(15):2026-33.

[20] He XD, Zhang FH, Wang RG, Liu WB. Preparation of a carbon nanotube/carbon fiber multi-scale reinforcement by grafting multi-walled carbon nanotubes onto the fibers. Carbon. 2007 Nov;45(13):2559-63.

[21] Zhang Q, Liu J, Sager R, Dai L, Baur J. Hierarchical composites of carbon nanotubes on carbon fiber: Influence of growth condition on fiber tensile properties. Composites Science and Technology. 2009;69(5):594-601.

[22] Qian H, Bismarck A, Greenhalgh ES, Shaffer MSP. Carbon nanotube grafted silica fibres: Characterising the interface at the single fibre level. Compos Sci Technol. 2009;doi:10.1016/j.compscitech.2009.11.014

[23] Sager RJ, Klein PJ, Lagoudas DC, Zhang Q, Liu J, Dai L, et al. Effect of carbon nanotubes on the interfacial shear strength of T650 carbon fiber in an epoxy matrix. Compos Sci Technol. 2009 Jun;69(7-8):898-904.

[24] Wu Z, Pittman JCU, Gardner SD. Nitric acid oxidation of carbon fibers and the effects of subsequent treatment in refluxing aqueous NaOH. Carbon. 1995;33:597-605.

[25] Downs WB, Baker RTK. Modification of the surface properties of carbon fibers via the catalytic growth of carbon nanofibers. J Mater Res. 1995;10:625-33.

[26] Song B, Bismarck A, Tahhan R, Springer J. A generalized drop length–height method for determination of contact angle in drop-on-fiber systems. J Colloid Interf Sci. 1998;197:68-77.

[27] Ho KKC, Kalinka G, Tran MQ, Polyakova NV, Bismarck A. Fluorinated carbon fibres and their suitability as reinforcement for fluoropolymers. Compos Sci Technol. 2007 Oct;67(13):2699-706.

[28] Kelly A, Tyson WR. Tensile properties of fiber-reinforced metals: copper/tungsten and copper/molybdenum. J Mech Phys Solids. 1965;13:329-50.

[29] Ohsawa T, Nakayama A, Miwa M, Hasegawa A. Temperature dependence of critical fiber length for glass fiber-reinforced thermosetting resins. J Appl Polym Sci. 1978;22(11):3203-12.

[30] Sinnott SB, Andrews R, Qian D, Rao AM, Mao Z, Dickey EC, et al. Model of carbon nanotube growth through chemical vapor depostion. Chem Phys Lett. 1999;315:25-30.

[31] Peng JCM, Donnet JB, Wang TK, Rebouillat S. Surface treatment of carbon fibers. In: Donnet JB, Wang TK, Rebouillat S, Peng JCM, eds. Carbon Fibers, 3rd Ed: Marcel Dekker, New York 1998:161-230.

[32] Ibarra L, Paños D. Carbon fibre oxidation, textural and surface changes Die Angewandte Makromolekulare Chemie. 2003;248(1):201-15.

[33] Pollack HW. Materials science and metallurgy, 4th ed.: Prentice-Hall 1988.

[34] Park SJ, Seo MK, Kim HY, Lee DR. Studies on PAN-based carbon fibers irradiated by Ar+ ion beams. J Colloid Interf Sci. 2003;261:393-8.

[35] Stoner EG, Edie DD, Durham SD. An end-effect model for the single-filament tensile test. J Mater Sci. 1994;29(Volume 29, Number 24 / January, 1994):6561-74.

[36] Carroll BJ. Equilibrium conformations of liquid-drops on thin cylinders under forces of capillarity - a theory for the roll-up process. Langmuir. 1986 Mar-Apr;2(2):248-50.

[37] McHale G, Newton MI, Carroll BJ. The shape and stability of small liquid drops on fibers. International Workshop on Wetting - From Microscopic Origins to Industrial Applications; 2000 May 06-12; Presquile De Giens, France: Editions Technip; 2000. p. 47-54.

[38] Neimark AV. Thermodynamic equilibrium and stability of liquid films and droplets on fibers. International Symposium on Apparent and Microscopic Contact Angles in Conjunction with the 216th American-Chemical-Society Meeting; 1998 Aug 24-27; Boston, Massachusetts: Vsp Bv; 1998. p. 1137-54.

[39] Tran MQ, Cabral JT, Shaffer MSP, Bismarck A. Direct measurement of the wetting behavior of individual carbon nanotubes by polymer melts: The key to carbon nanotube-polymer composites. Nano Letters. 2008 Sep;8(9):2744-50.

[40] Wenzel RN. Surface roughness and contact angle. J Phys Colloid Chem. 1949;53:1466-7.

[41] Hsieh C-T, Chen J-M, Kuo R-R, Lin T-S, Wu C-F. Influence of surface roughness on water- and oil-repellent surfaces coated with nanoparticles. Applied Surface Science. 2005;240(1-4):318-26.

[42] Wolansky G, Marmur A. Apparent contact angles on rough surfaces: the Wenzel equation revisited. Colloid Surf A-Physicochem Eng Asp. 1999 Oct;156(1-3):381-8.

[43] Feih S, Wonsyld K, Minzari D, Westermann P, Lilholt H. Testing procedure for the single fiber fragmentation test. Roskilde: Risø National Laboratory; 2004. Report No.: Risø-R-1483(EN).

Table 1

Single fibre tensile test results for the IM7 carbon fibres, determined at different gauge lengths. The standard errors are shown in the brackets.

Fibre	Gauge length (mm)	Tensile strength (MPa)	Tensile modulus (GPa)
as-received	15	5890 (*160*)	298 (*3*)
	25	5650 (*190*)	298 (*1*)
	35	4840 (*160*)	299 (*1*)
oxidised	15	6260 (*170*)	300 (*2*)
	25	6080 (*180*)	296 (*1*)
	35	5150 (*220*)	299 (*1*)
CNT-grafted	15	4950 (*170*)	292 (*3*)
	25	4670 (*180*)	287 (*1*)
	35	4000 (*180*)	291 (*1*)

Table 2

Weibull distribution parameters and single fibre fragmentation test results for the IM7 carbon fibres determined through single fibre fragmentation tests. The fibre tensile strengths at critical length are predicted from the Weibull distribution. The standard errors are shown in parentheses.

fibres	m	σ_0 (MPa)	σ_f (MPa)	d_f (μm)	l_c (μm)	τ_{IFSS} (MPa)
as-received	8.81	8270	7360	5.2	1750 (*40*)	12.5 (*0.2*)
oxidised	9.65	8520	7690	5.2	1650 (*30*)	13.1 (*0.2*)
CNT-grafted	6.45	7910	7070	5.2	1310 (*40*)	15.8 (*0.4*)

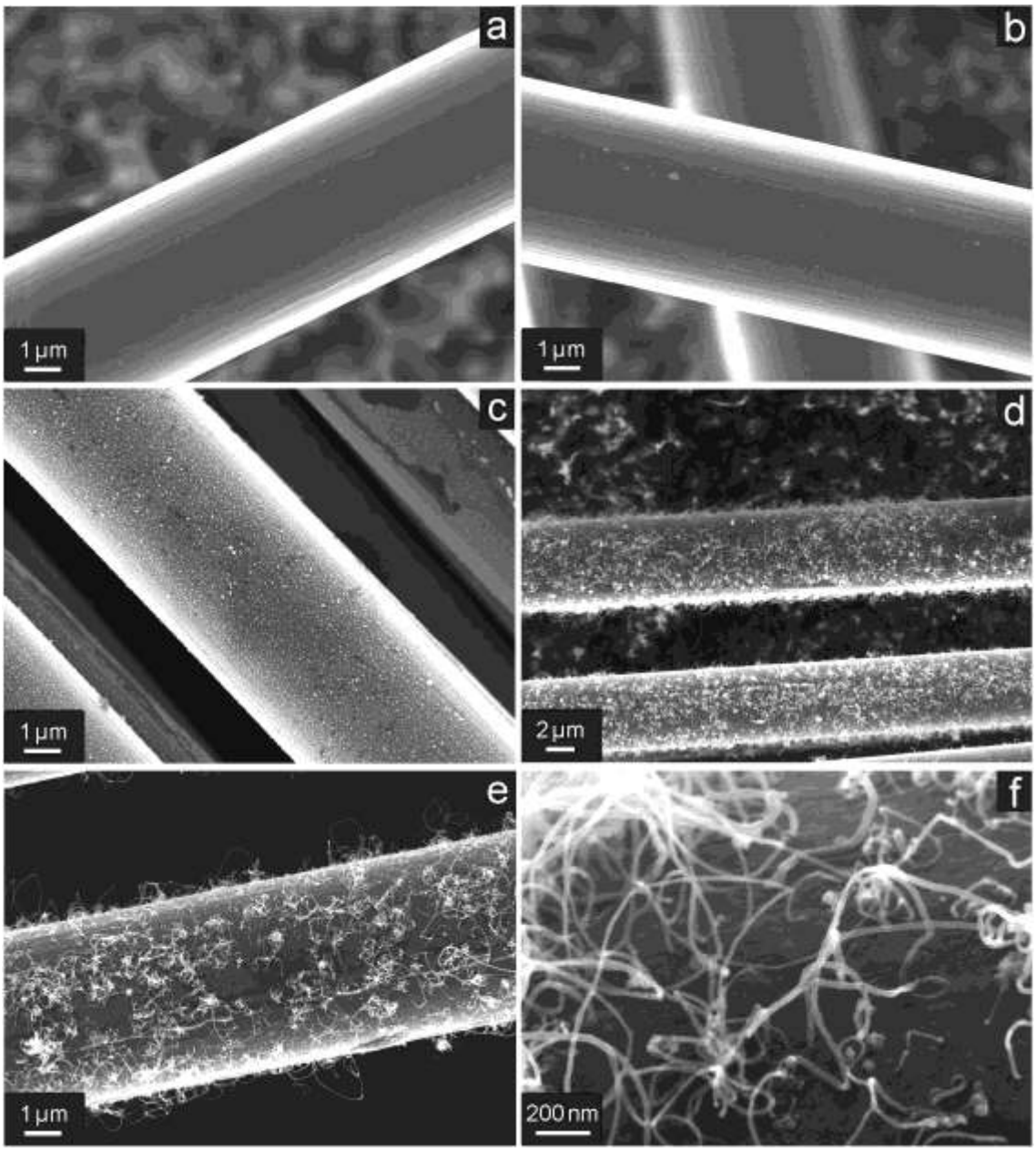

Fig. 1: SEM images of (a) as-received IM7 carbon fibres after (b) oxidation, (c) catalyst deposition and (d)-(f) growth of CNTs using the CVD method.

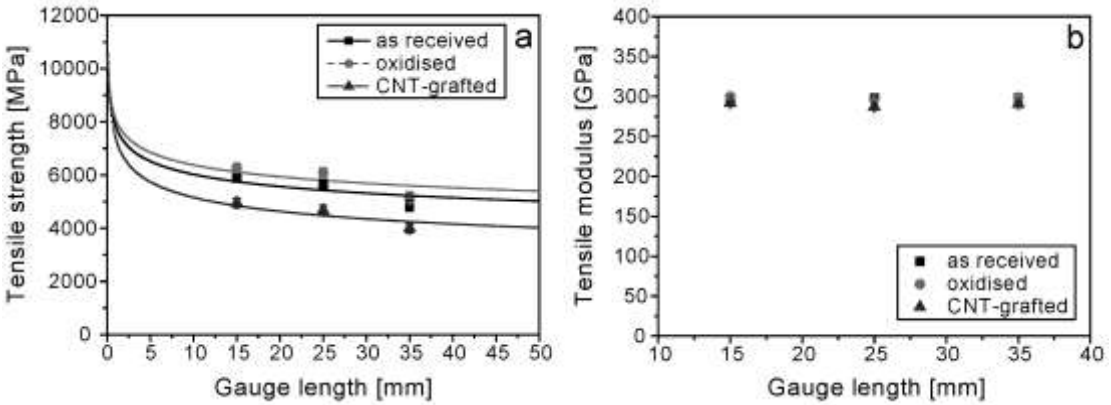

Fig. 2. Single fibre tensile data: (a) strength and (b) modulus plotted as a function of gauge length for the IM7 carbon fibres. The Weibull distribution (shown as lines) in (a) was used to account for the gauge length dependence of the tensile strength.

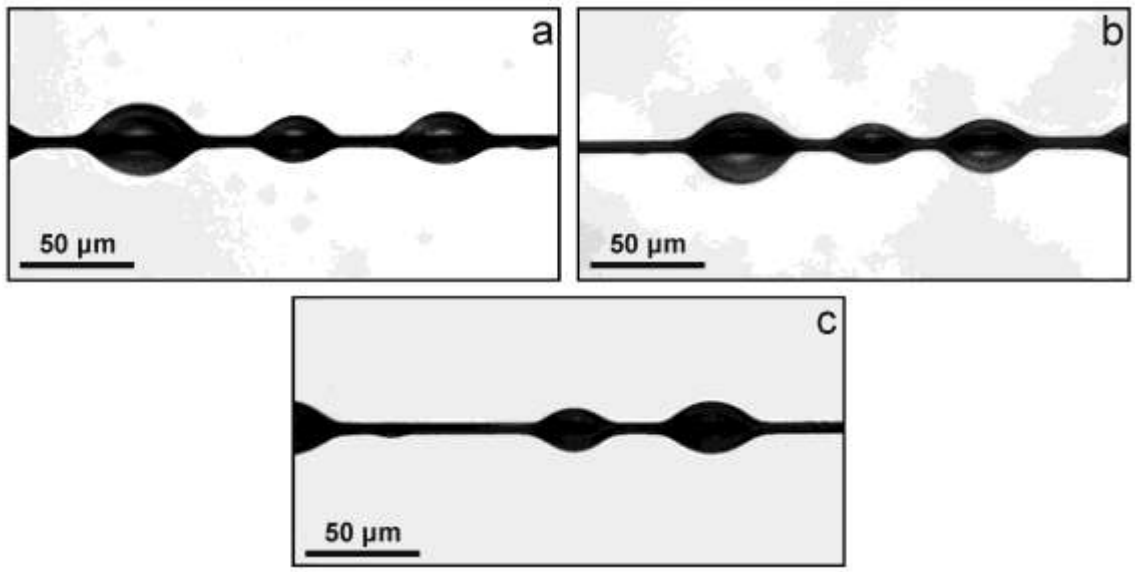

Fig. 3. Optical micrographs of typical PMMA droplets formed on (a) as-received, (b) oxidised and (c) CNT-grafted IM7 carbon fibres.

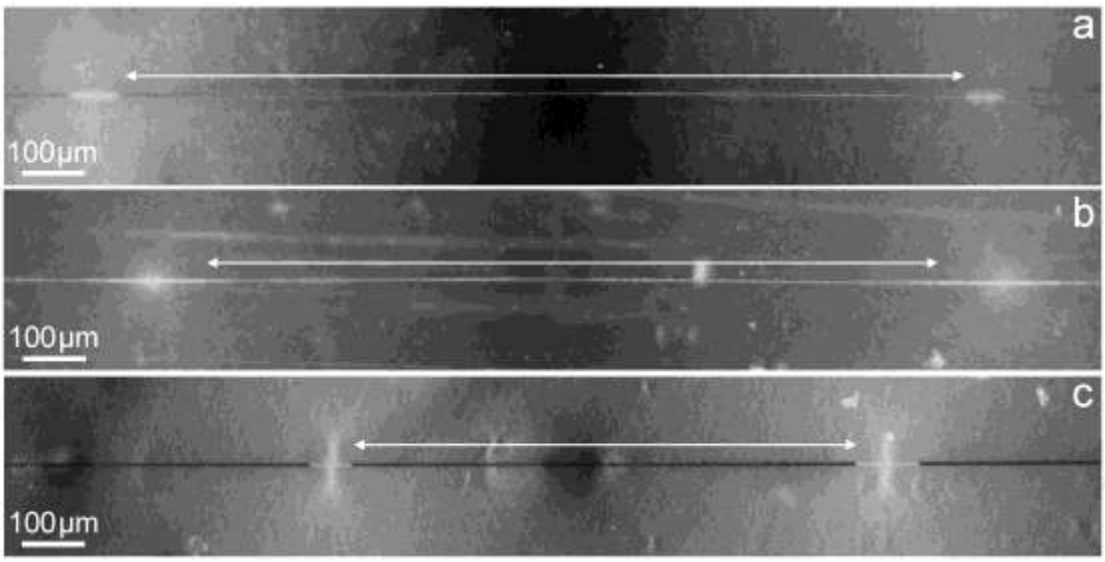

Fig. 4: Typical dark field optical micrographs of (a) as-received (b) oxidised and (b) CNT-grafted IM7 carbon fibre breaks in PMMA matrix after the fragmentation test. The bright areas represent the cracks and the arrows indicate the fragment length.

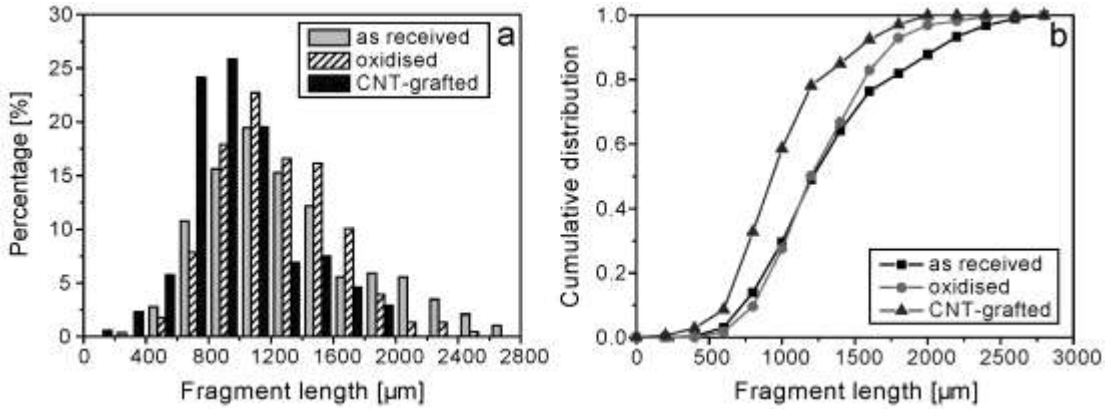

Fig. 5: (a) Histogram and (b) cumulative distributions of fragment lengths for the IM7 carbon fibres.

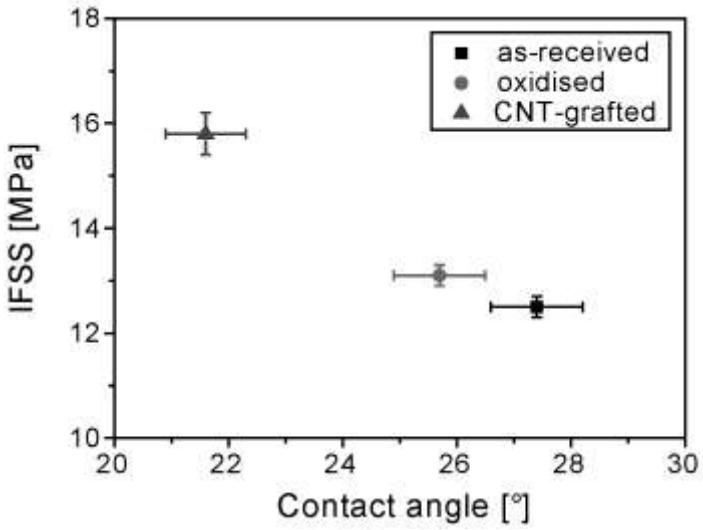

Fig. 6. Apparent IFSS plotted as a function of contact angle, using PMMA as a model matrix.

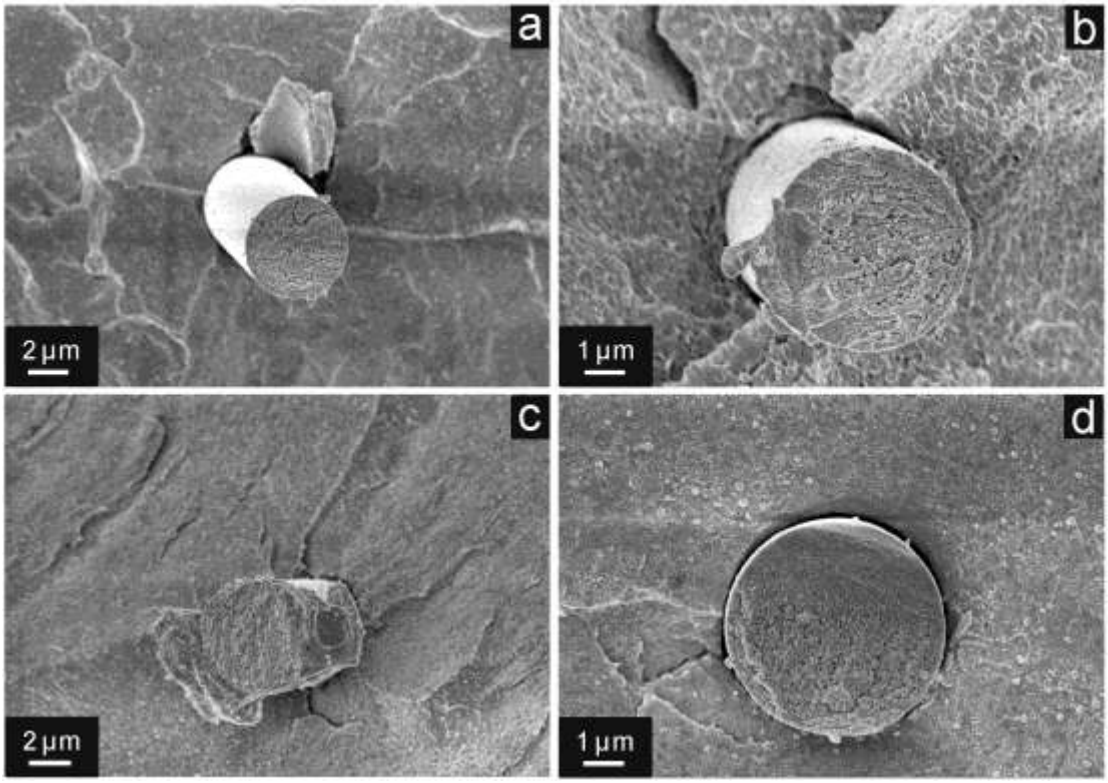

Fig. 7. SEM images of the fracture surfaces of the IM7 carbon fibre/PMMA composites (a), (b) without and (c), (d) with CNTs grafted on the fibres.

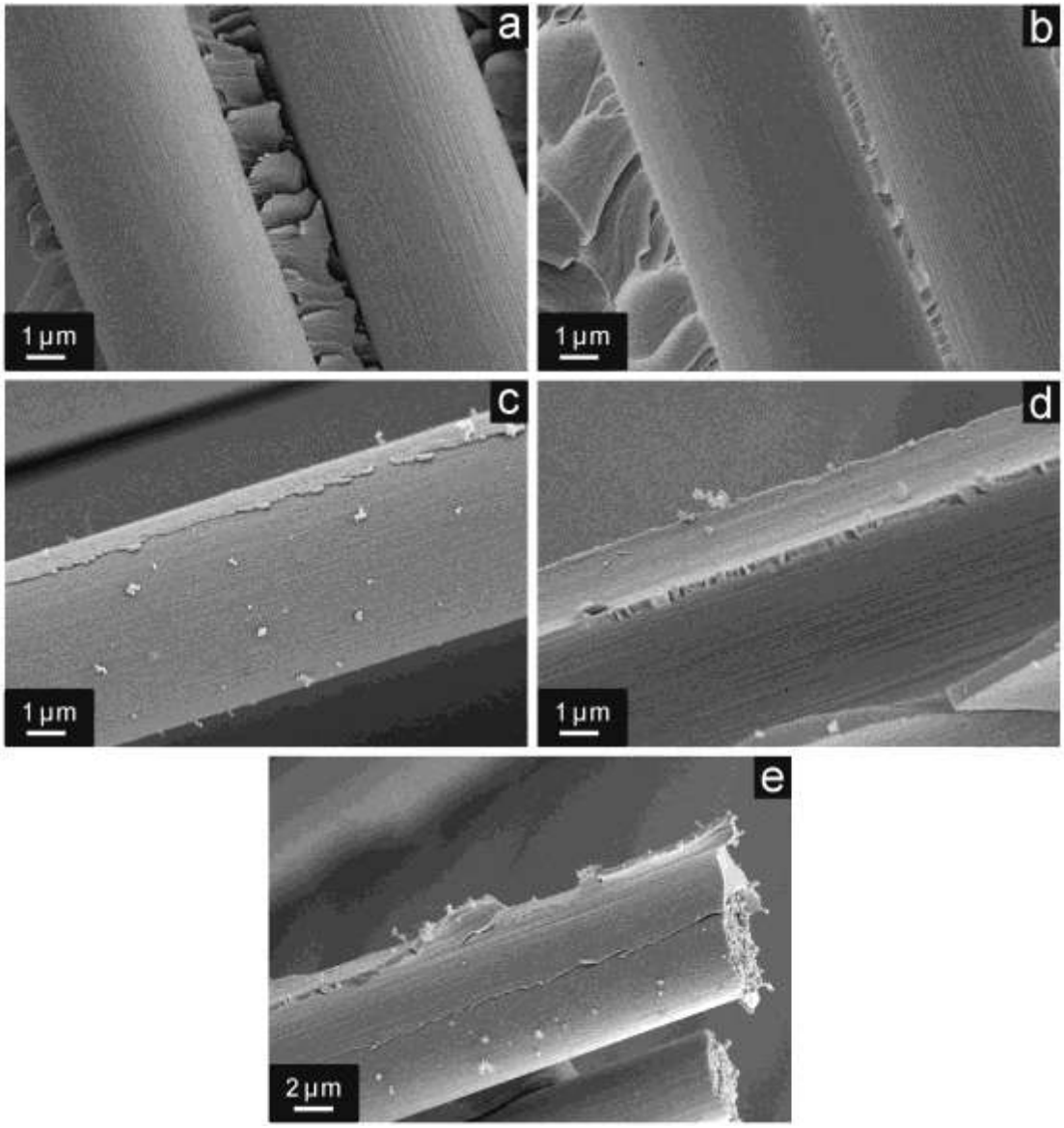

Fig. S1. Typical SEM images of the fracture surfaces of the IM7 carbon fibre/epoxy composites (a), (b) without and (c) - (e) with CNTs grafted on the fibres. Fracture planes lay between fibres and matrix in both cases. A few nanoparticles were found on the fibre surfaces in (c), which could be attributed to the residue catalyst particles after the fracture. CNTs that extend into the matrix around the fibres were clearly shown in (d) and (e).